Chinese Chemical Letters 33 (2022) 1619–1622

Contents lists available at ScienceDirect

Chinese Chemical Letters

journal homepage: www.elsevier.com/locate/cclet

Virus-inspired nanoparticles as versatile antibacterial carriers for antibiotic delivery against Gram-negative and Gram-positive bacteria

Kefurong Deng, Yachao Li*, Xiaoyu Liang, Cheng Shen, Zenan Zeng, Xianghui Xu*

Department of Pharmacy, College of Biology, Hunan University, Changsha 410082, China

ARTICLE INFO

Article history:
Received 15 June 2021
Revised 10 September 2021
Accepted 13 September 2021
Available online 20 September 2021

Keywords:
Virus-inspired nanoparticles
Bacterial intracellular drug delivery
Antibacterial treatment
Gram-positive bacteria
Gram-negative bacteria

ABSTRACT

Infectious diseases become one of the leading causes of human death. Traditional treatment based on classical antibiotics could not provide enough antibacterial activity to combat bacterial infections due to low bioavailability, even leading to antibiotic resistance. In recent years, biomimetic delivery systems have been developed to improve drug therapy for various diseases, such as malignant tumor and cardiovascular disease. In this work, we designed virus-inspired nanodrugs (VNDs) through co-assembly of amphiphilic lipopeptide dendrons and poly(lactic-*co*-glycolic acid) polymers for high-efficiency antibiotic delivery. These VNDs had well-defined and stable nanostructures for tetracycline encapsulation and delivery. The VNDs were capable of promoting antibiotic internalization and enhancing their antibacterial effects against Gram-negative *Escherichia coli* and Gram-positive *Staphylococcus aureus*. Additionally, no obvious cytotoxicity of VNDs was observed to human cell lines. This work successfully demonstrated the virus-mimetic nanoparticles served as promising and applicable antibiotic delivery platform for antibacterial treatment.

Infectious diseases become an increasing threat to human health. It is reported that by 2050 serious infections will kill 10 million people per year, more than that of malignant tumors [1]. Thereinto, bacterial infections account for the majority of infectious diseases, and how to effectively combat bacterial infectious is one of hottest spots in biomedical field. Diverse pharmaceutical molecules have been created for antibacterial therapy through one or more of the known mechanisms as follows: inhibiting biosynthesis of (i) bacterial cell wall (*e.g.*, penicillin, vancomycin and daptomycin), (ii) bacterial protein (*e.g.*, tetracycline, tobramycin and erythromycin), (iii) bacterial nucleotides (*e.g.*, ciprofloxacin, rifampin, and cotrimoxazole), and (iv) disturbing cell membrane (*e.g.*, polymyxins) [2,3]. Most of the antibiotics exert antibacterial effects in bacterial cytoplasm, especially for biosynthesis-inhibiting drugs. However, undesirable physicochemical properties (*e.g.*, poor water solubility) and indurative bacterial barriers (including cell walls and membranes) tremendously reduce antibiotic bioavailability and antibacterial efficacy [4,5]. Moreover, traditional ways for promoting antibacterial effects often lead to side effects and antibiotic resistance, such as increasing antibiotic dose and administration frequency [6]. Therefore, enhancing antibiotic bioavailability and antibacterial effects remains an enormous challenge.

In recent years, nanomedicine solutions emerge great potentials for addressing the defects of antibiotics in antibacterial therapy [7–13]. Tailoring nanoparticles is able to harbor antibiotics, improve their property, enhance bacterial internalization, deliver in bacterial cytoplasm and finally maximize antibacterial activity [14–16]. For examples, biodegradable antibiotic-loaded nanoparticles based on China National Medical Products Administration (NMPA)-approved poly(lactic-*co*-glycolic acid) (PLGA) polymers succeeded in improving the effectiveness of the antibiotics, revealing the huge potentials on clinical transformation [17–19]. Among the multitudinous nanocarriers, virus-inspired nanoparticles (VNPs) have brought about widespread attentions on the development of advanced drug delivery systems, owing to their outstanding ability for improving drug bioavailability [20,21]. Previously, we successfully designed a series of virus-inspired nanocarriers for robust antitumor drug delivery, allowing for overcoming sequential barriers, deep tissue penetration and site-specific molecular delivery [22–28]. Moreover, hybrid VNPs assembled from human papillomavirus capsid protein L1 could increase activity of polyoxometalates against *E. coli* bacteria, and hybrid VNPs composed of mesoporous silica-coated plasmonic Ag nanocube could optimize gentamicin delivery for antibacterial eradication of diabetic wound ulcer healing [29]. Although these hybrid VNPs indeed im-

* Corresponding authors.
E-mail addresses: yachao_li@hotmail.com (Y. Li), xianghui.xu@hnu.edu.cn, xianghui.xu@hotmail.com (X. Xu).

https://doi.org/10.1016/j.cclet.2021.09.045
1001-8417/

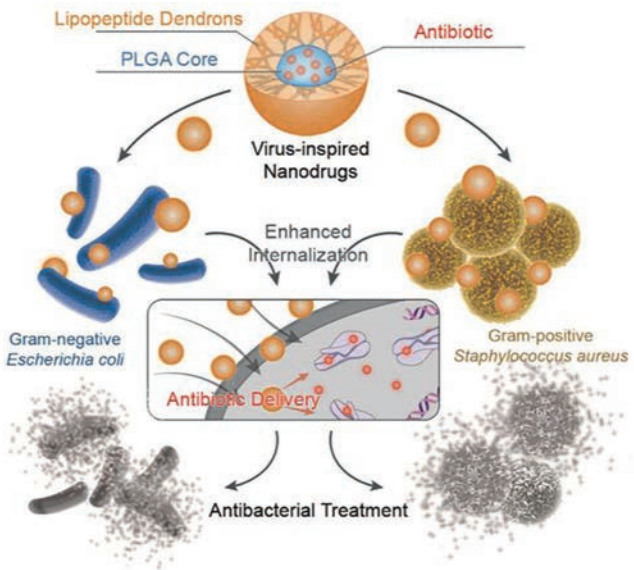

Scheme 1. Schematic illustration of VNDs for antibiotic delivery against Gram-negative and Gram-positive bacteria.

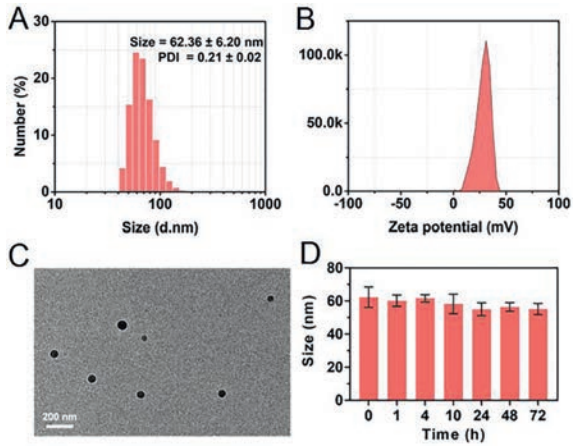

Fig. 1. Nanostructure characterizations of VNDs. (A) Hydrodynamic size distribution and (B) zeta potential of VNDs determined by DLS. (C) TEM image of VNDs. (D) Size stability of VNDs in PBS at room temperature for 72 h (means ± standard deviation (SD), $n = 3$).

Table 1
Antibacterial activity of free Tet, VNDs and FPNDs.

Compounds	*E. coli*		*S. aureus*	
	MIC_{24h}	MIC_{48h}	MIC_{24h}	MIC_{48h}
Free Tet	8	>16	0.5	2
VNDs	1	1	0.5	0.5
FPNDs	2	>16	0.5	1

MIC is defined as the minimum drug concentration (μg/mL) that completely inhibits bacteria growth.

prove antibiotic bioavailability and curative efficiency, their complicated components and nanostructures seriously influence biological safety, biocompatibility, controllable preparation and clinical applications of these VNPs [30]. For these reasons, developing efficient VNPs with practicable strategy for antibiotic delivery is highly pursued for treatment of infectious diseases.

In this work, we developed VNPs through co-assembly of amphiphilic lipopeptide dendrons (LPDs) and PLGA polymers as versatile antibacterial nanocarriers for antibiotic delivery (Scheme 1). Amphiphilic LPDs with abundant lysine residues imitated architectures and components of natural globular proteins, and these LPDs could spontaneously assemble into capsid-like nanostructures. Meanwhile, the hydrophobic PLGA could aggregate at inner core of capsid-like nanostructures as stable pockets for drug loading. The VNPs hold great potentials to efficiently encapsulate antibiotics and enhance antibiotic internalization into bacteria. Tetracycline (Tet) as a first-line antibiotic was selected as a drug model in this study, owing to its broad-spectrum antibacterial activity. Tet-loaded VNPs was termed as virus-inspired nanodrugs (VNDs), which was expected to improve antibiotic bioavailability *in vitro* and antibacterial effects on Gram-positive and Gram-negative bacteria.

In the first place, amphiphilic LPDs was synthesized by a divergent approach, and the detailed synthetic procedures and characterizations can be found in Supporting information (Schemes S1−S3 and Figs. S1−S6). Then, VNDs were prepared by supramolecular assembly in a phosphate buffered solution. Briefly, PLGA and Tet were fully dissolved in acetone, and LPDs were dispersed in buffered solution. Under vigorous stirring, the mixture solution (PLGA and Tet) was dropwise added into LPDs solution to fabricate VNDs. After stirring for 4 h, the solution was purified with dialysis (MWCO 2000) in deionized water, and VNDs could be obtained by vacuum freeze-drying. In addition, classical pluronic F68-coated PLGA nanoparticles (FPNPs) and Tet-loaded FPNPs (FPNDs) were prepared as control groups, using the same method [31]. The dynamic light scattering (DLS) results indicated VNDs had an average size of 62.36 ± 6.18 nm with a good polydispersity index (PDI), and zeta potential of VNDs was +25.9 mV (Figs. 1A and B, Figs. S7 and S8 in Supporting information). Transmission electron microscopy (TEM) image revealed that these VNDs presented uniform spherical nanostructures with size around 50 nm (Fig. 1C). Drug loading capacity and drug-loading efficiency were 6.62% and 33.00%, respectively. Moreover, VNDs could stably exist in normal physiological conditions without evident dimensional change around 60 nm for 72 h (Fig. 1D and Fig. S9 in Supporting information). Taken together, VNDs had well-defined and stable structures for encapsulating hydrophobic antibiotics, and their positively-charged surface could increase the interactions between VNDs and negatively-charged bacteria as well as promote antibacterial treatment.

Once successful fabrication of VNDs was confirmed, we started to investigate the antibacterial activity against Gram-negative and Gram-positive bacteria. As shown in Fig. 2A, VNDs with Tet concentration of 1 μg/mL could powerfully inhibit the growth of Gram-negative bacteria of *Escherichia coli* (*E. coli*), while free Tet provided antibacterial activity against at the concentration of 8 μg/mL. As the incubation time went on to 48 h, VNDs invariably showed efficient antibacterial activity, but free Tet was not able to inhibit *E. coli* at the highest concentration of 16 μg/mL. At the same time, antibacterial activities of VNDs against *E. coli* were much better than those of FPNDs with different incubation time. VNDs also demonstrated the most effective antibacterial activity against Gram-positive bacteria of *Staphylococcus aureus* (*S. aureus*), as compared with free Tet and FPNDs at the incubation time of 24 h and 48 h (Fig. 2B). These results suggested virus-inspired nanocarriers were capable of enhancing the antibacterial activity of antibiotic, much better than the classical carriers of F68-coated PLGA nanoparticles.

To directly present antibacterial activities of these agents, their minimum inhibition concentrations (MIC) were summarized in Table 1, which is defined as the minimum drug concentration for completely inhibiting bacteria growth. The MIC value of VNDs against *E. coli* decreased 8 times, as compared with free Tet at the incubating time of 24 h. Moreover, VNDs still maintained a

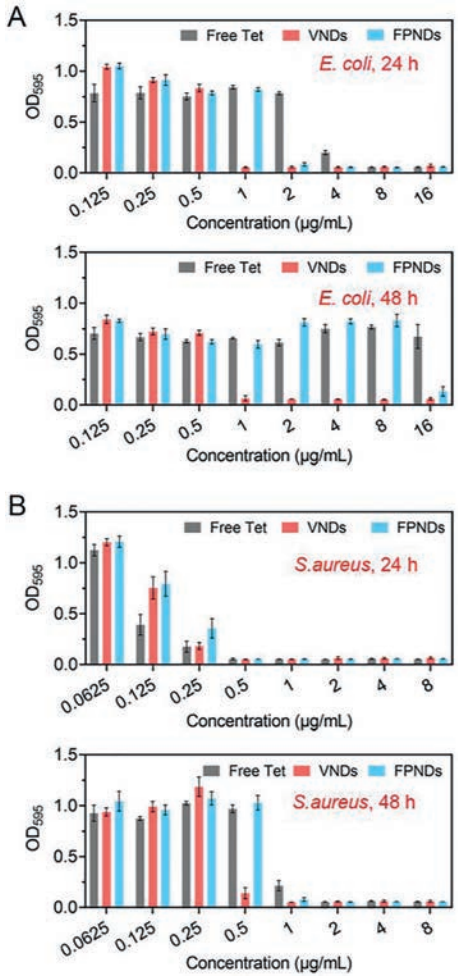

Fig. 2. Antibacterial efficacy of VNDs. Growth inhibition of (A) *E. coli* and (B) *S. aureus* in the presence of free Tet, VNDs and FPNDs with different Tet concentration for 24 h and 48 h, respectively (means ± SD, $n = 3$).

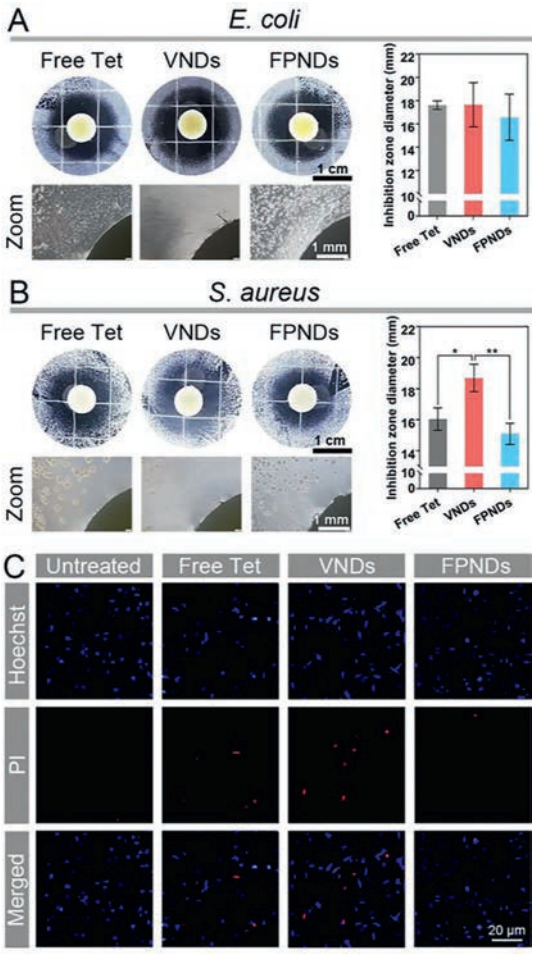

Fig. 3. Bacterial inhibition zone images, microscope images and inhibition zone diameter after treatment with free Tet, VNDs and FPNDs with Tet dosage of 5.12 μg against (A) *E. coli* and 1.28 μg against (B) *S. aureus*. (C) Fluorescent images for *E. coli* after treatment with free Tet, VNDs and FPNDs at the Tet concentration of 0.5 μg/mL for 2 h.

low MIC value of 1 μg/mL against *E. coli* for 24 h, while free Tet could not efficiently inhibit *E. coli* even at a high concentration of 16 μg/mL. This result further confirmed bioinspired design of Tet-loaded nanodrugs dramatically raised antibacterial effects against Gram-negative bacteria. Likewise, VNDs also showed highly efficient antibacterial activity against Gram-positive bacteria of *S. aureus* after 48 h treatment. Additionally, VNPs without Tet did not show influence on Gram-negative and Gram-positive bacteria at the corresponding concentration of MIC value (Figs. S10 and S11 in Supporting information). Altogether, virus-inspired nanodrugs displayed excellent and long-term antibacterial capability against Gram-negative and Gram-positive bacteria.

Next, we visually investigated the antibacterial effects of VNDs using the agar diffusion method. As shown in Fig. 3A, there was no distinct difference on the diameters of inhibition zones among the *E. coli* groups after treatment with free Tet, VNDs and FPNDs, whereas many bacteria still could be observed in inhibition zones of Tet-treated or FPNDs-treated groups but few bacteria could be found in the VNDs-treated group in microphotographs. As for antibacterial effects against *S. aureus*, VNDs-treated group had the widest diameter of inhibition zone comparing with the Tet-treated or FPNDs-treated groups, and the least bacteria were observed by microscope (Fig. 3B). These results consistently showed that VNDs largely elevated the antibacterial effects of antibiotic.

To further verify the antibacterial performance of VNDs, we employed propidium iodide (PI) staining to visualize the damage of bacterial cell through inverted fluorescence microscope. DNA-specific fluorescent dye of Hoechst 33342 stained all bacteria with blue fluorescence, whereas PI only stained dead bacterial with red fluorescence due to permeabilized inner membranes [32]. As shown in Fig. 3C, after treatment with 0.5 μg/mL antibacterial agents for 2 h, the most PI-positive bacteria could be watched in the VNDs-treated group, suggesting significant death of bacteria. The aforementioned results manifested VNDs successfully overcame poor efficiency of conventional antibiotics and revealed satisfactory antibacterial activity against Gram-negative and Gram-positive bacteria.

To disclose the mechanisms on high-efficiency antibacterial effects of VNDs, we analyzed the Tet internalization into bacterial cytoplasm using confocal laser scanning microscope (CLSM). *E. coli* were treated with different drug formulations at the Tet concentration of 0.5 μg/mL for 4 h. Tet could be imaged by its inherent fluorescence with green color by CLSM. As shown in Fig. 4, a small amount of free Tet was taken into bacteria, and nanoformulation of FPNDs could enhance the bacterial uptake of Tet. Attractively, VNDs prominently facilitate antibiotic internalization, owing to the virus-mimicking components and nanostructures with positively-charged surface. Thus, it can be seen that virus-inspired nanodrugs contributed to the improvement on bacterial uptake of antibiotics, exerting maximum inhibition activity on protein biosynthesis.

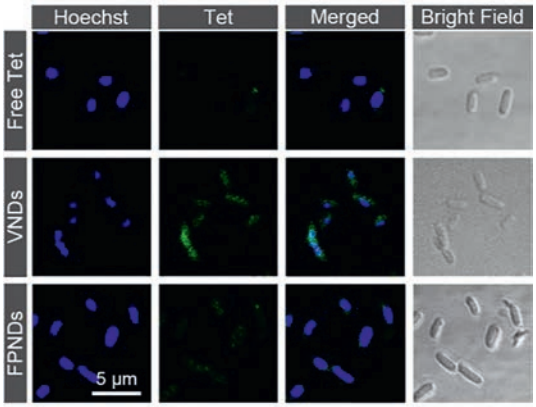

Fig. 4. Bacterial internalization of VNDs. CLSM images for *E. coli* after incubation with free Tet, VNDs and FPNDs at the concentration of 0.5 μg/mL for 4 h, including Hoechst 33342 stained DNA channel (blue) and Tet channel (green). For interpretation of the references to color in this figure legend, the reader is referred to the web version of this article.

Subsequently, we evaluated cytotoxicity of these formulations to normal human cell lines at the effective bacteriostatic concentration using CCK-8 assay. The results clearly revealed that VNDs had no obvious toxicity to human umbilical vein endothelial cells (HUVEC) and smooth muscle cells (SMC) at a Tet concentration of 2 μg/mL (4-fold of MIC value of *S. aureus* and 2-fold of MIC value to *E. coli*) for 48 h (Figs. S12−S22 in Supporting information). In the meantime, the bioinspired delivery system of VNPs also showed no apparent toxicity to both HUVEC and SMC. It was indicated that the bioinspired delivery system of VNDs was an efficient and biocompatible antibacterial agent.

In summary, virus-inspired nanodrugs was developed to achieve high-efficiency antibacterial activity against Gram-negative and Gram-positive bacteria. These VNDs had well-organized and stable nanostructure and nanostructure mimicking with positively-charged corona of lipopeptide dendrons and inner PLGA core. These nanoparticles could encapsulate antibiotic and enhance bacterial internalization. Remarkable bacterial uptake and accumulation of antibiotic facilitated very high antibacterial effects against *E. coli* and *S. aureus*. More importantly, VNDs did not show cytotoxicity to normal human cell lines at the effective antibacterial concentration. This work puts forward a promising and feasible strategy on molecular and supramolecular development of efficien antibacterial nanodrugs for combat infectious diseases.

Declaration of competing interest

The authors declare no conflict of interest.

Acknowledgments

This work was supported by National Natural Science Foundation of China (NSFC, Nos. 91956105, 22077028 and 32000995), China National Postdoctoral Program for Innovative Talents (No. BX20200124), China Postdoctoral Science Foundation (No. 2020M682544), the Fundamental Research Funds for the Central University (No. 531118010440) and Major Research Projects (No. 531118100003) from Hunan University.

Supplementary materials

Supplementary material associated with this article can be found, in the online version, at doi:10.1016/j.cclet.2021.09.045.

References

[1] WHO, No time to wait: Securing the future from drug-resistant infections, https://www.who.int/antimicrobial-resistance/interagency-coordination-group/final-report/en/ (accessed April 2019).
[2] M.A. Kohanski, D.J. Dwyer, J.J. Collins, Nat. Rev. Microbiol. 8 (2010) 423–435.
[3] W. Li, F. Separovic, N.M. O'Brien-Simpson, J.D. Wade, Chem. Soc. Rev. 50 (2021) 4932–4973.
[4] W. Gao, S. Thamphiwatana, P. Angsantikul, L. Zhang, WIREs Nanomed. Nanobiotechnol. 6 (2014) 532–547.
[5] S. Menina, J. Eisenbeis, M.A.M. Kamal, et al., Adv. Healthcare Mater. 8 (2019) 1900564.
[6] M.H. Xiong, Y. Bao, X.Z. Yang, et al., Adv. Drug Delivery Rev. 78 (2014) 63–76.
[7] K. Dillen, C. Bridts, P. Van der Veken, et al., Int. J. Pharm. 349 (2008) 234–240.
[8] C. Liu, H. Shen, S. Wang, et al., Chin. Chem. Lett. 29 (2018) 1824–1828.
[9] M. Yousefi, A. Ehsani, S.M. Jafari, Adv. Colloid Interface Sci. 270 (2019) 263–277.
[10] Y. Liu, D. Li, J. Ding, X. Chen, Chin. Chem. Lett. 31 (2020) 3001–3014.
[11] Y. Zheng, H. Jiang, X. Wang, Chin. Chem. Lett. 31 (2020) 3183–3189.
[12] X. Huang, W. Xu, M. Li, et al., Matter 4 (2021) 1892–1918.
[13] J. Zhang, C. Xiao, X. Zhang, et al., J. Control. Release 335 (2021) 359–368.
[14] M.J. Hajipour, K.M. Fromm, A. Akbar Ashkarran, et al., Trends Biotechnol 30 (2012) 499–511.
[15] S. Fulaz, S. Vitale, L. Quinn, E. Casey, Trends Microbiol. 27 (2019) 915–926.
[16] C.H. Li, X. Chen, R.F. Landis, et al., ACS Infect. Dis. 5 (2019) 1590–1596.
[17] U.S. Toti, B.R. Guru, M. Hali, et al., Biomaterials 32 (2011) 6606–6613.
[18] F. Danhier, E. Ansorena, J.M. Silva, et al., J. Control. Release 161 (2012) 505–522.
[19] Y. Zhou, A. Fang, F. Wang, et al., Chin. Chem. Lett. 31 (2020) 494–500.
[20] A. Parodi, R. Molinaro, M. Sushnitha, et al., Biomaterials 147 (2017) 155–168.
[21] Y. Chen, X. Li, M. Wang, et al., Small 16 (2020) 1906028.
[22] X. Xu, Y. Jian, Y. Li, et al., ACS Nano 8 (2014) 9255–9264.
[23] Z. Zhang, X. Zhang, X. Xu, et al., Adv. Funct. Mater. 25 (2015) 5250–5260.
[24] Y. Li, X. Xu, X. Zhang, et al., ACS Nano 11 (2017) 416–429.
[25] Y. Li, X. Zhang, Z. Zhang, et al., Mater. Horiz. 5 (2018) 1047–1057.
[26] X. Zhang, X. Xu, Y. Li, et al., Adv. Mater. 30 (2018) 1707240.
[27] Y. Li, X. Xu, J. Control. Release 323 (2020) 483–501.
[28] Q. Xu, C. Shu, Y. Li, et al., Chem. Commun. 57 (2021) 4859–4862.
[29] P. Wang, S. Jiang, Y. Li, et al., Nanomedicine NBM 34 (2021) 102381.
[30] G. Yang, S.Z.F. Phua, A.K. Bindra, Y. Zhao, Adv. Mater. 31 (2019) 1805730.
[31] M.N.V. Ravi Kumar, U. Bakowsky, C.M. Lehr, Biomaterials 25 (2004) 1771–1777.
[32] S.E. Birk, A. Boisen, L.H. Nielsen, Adv. Drug Delivery Rev. 174 (2021) 30–52.